

## Residual Stresses Near Holes In Tempered Glass Plates

Laurent Daudeville<sup>1</sup>, Fabrice Bernard<sup>2</sup> and René Gy<sup>3</sup>

<sup>1</sup> Laboratoire Sols, Solides, Structures, DU, BP 53, 38041 Grenoble Cedex 9, France

<sup>2</sup> ENS Mines de Douai, Dpt génie civil, BP 838, 59508 Douai Cedex, France

<sup>3</sup> Saint-Gobain Recherche, BP 135, 93303 Aubervilliers Cedex, France

**Keywords:** tempered glass, structural glass, residual stresses, thermal transfers, photo-elasticity.

**Abstract.** This work presents numerical simulation results of the thermal tempering by the Finite Element Method in order to calculate transient and residual stresses near edges of a glass plate (2D calculation) and near holes (3D calculation). During thermal tempering, glass is considered as a viscoelastic material. The Narayanaswamy's model is used. It takes into account the structural relaxation phenomena. The particular difficulty is the correct modelling of heat transfers since transient and residual stresses strongly depend on the history of temperature within the plate, close to the edge and the hole. Both the forced convection due to the blowing of air and the radiative heat transfer are modelled numerically. The semi-transparency of glass in the near infrared range is considered. The convective heat transfer coefficients on the edge and hole walls are identified thanks to a specific experimental set-up and validated from simulations of heat transfer tests. The computed residual stresses are checked against photo-elastic measurements.

### Introduction

In the design of high load bearing capacity beams made of tempered flat glass, connections cannot be avoided when long beams or inertia beams are considered. The studied technology is derived from the one used for hung glass, for the façades for example. In such structural applications, glass plates are loaded through metallic dowel type joints. This metallic connector is inserted in a chamfered hole of the glass plate (Fig. 1).

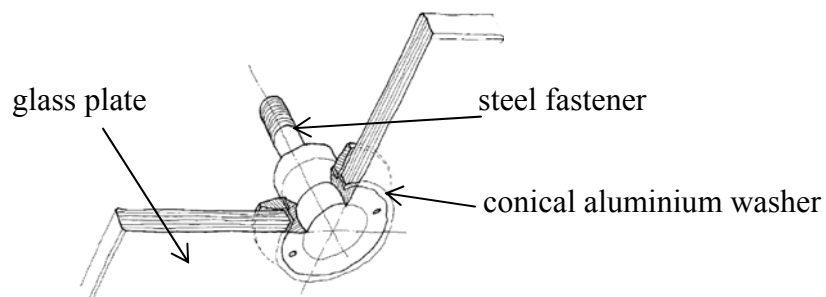


**Fig. 1.** Schematic view of a mechanical joint in a tempered glass plate

The first stage of the study is the calculation of the residual stresses in the vicinity of the chamfered hole (3D calculation). Previous analysis of glass tempering have been concerned with the calculation of residual stresses in infinite plates, i.e. far away from edges and possible holes, by means of a 1D modelling [1]. The computation of residual stresses in the vicinity of a straight edge (2D modelling) was carried out in [2] and near holes in [3], but these previous analyses were not taking into account, in an exhaustive way, the heat transfers occurring during the tempering process.

The presented contribution concerns the prediction of transient and residual stresses, not only close to straight edges, but also in the vicinity of chamfered holes of 19 mm thick glass plates. A thermo-mechanical calculation is carried out with the Finite Element Method (FEM). The

knowledge of both the mechanical behaviour of glass and the temperature history in the whole plate during the tempering process are then necessary.

This paper focuses on the identification of the different heat exchanges for a correct modelling of the tempering process. Several hole geometries are considered: large, mean and small 45° chamfers. Finally, this study allows us to determine which hole geometry of hole gives the best reinforcement.

### Description of the holed plates

The considered glass is a 19 mm thick Planilux glass produced by Saint-Gobain. For such structural applications, glass plates are loaded in their plane, chamfered holes are then symmetrical. The fabrication was carried out by Saint-Gobain. Five different geometries were studied (Fig. 2, Table 1).

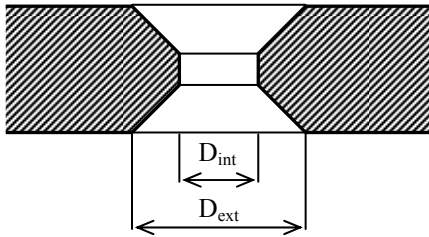


**Fig. 2.** Chamfered holes

Designation	$D_{int}$ (mm)	$D_{ext}$ (mm)
a1	38	40
a2	54	56
b1	24	40
b2	40	56
c1	30	40

**Table 1.** The five different studied geometries

### Mechanical behavior

During tempering, the behavior of glass varies quickly around the transition temperature ( $T_g \approx 580^\circ\text{C}$ ) between the “glass” and “liquid” states. In the transition zone, glass is a viscoelastic and thermorheologically simple material. The structural relaxation phenomenon has to be taken into account in the modelling of the quenching process. This mechanical behaviour was widely studied in the literature. Narayanaswamy [4] proposed a model that includes both structural and viscous relaxation phenomena. The Narayanaswamy’s model was implemented in the software Abaqus for the present study.

**Linear viscoelastic behavior of glass.** The temperature is first considered as constant. The viscoelastic behaviour is described in terms of stress relaxation by means of a generalised Maxwell model. The bulk part is separated from the deviatoric one. Relaxation shear ( $G$ ) and bulk moduli ( $K$ ) are described with instantaneous and deferred moduli and expanded into Prony’s series of six terms [5]. The deferred shear modulus value is zero.

$$G(t) = 2G_g \Psi_1(t) \text{ and } K(t) = 3K_e - (3K_e - 3K_g) \Psi_2(t). \quad (1)$$

$$\text{with } \Psi_i(t) = \sum_{j=1}^{n_i} w_{ij} \exp\left(-\frac{t}{\tau_{ij}}\right) \quad i = 1, 2. \quad (2)$$

**Thermorheological simplicity.** The thermorheological simplicity feature consists in considering that temperature ( $T$ ) and time ( $t$ ) are two dependant state variables. Indeed relaxation functions have the same form for different temperatures; they are only translated along the temperature scale. Thus, the knowledge of the glass behaviour at a reference temperature allows its knowledge at any other temperature by the intermediary of the reduced time ( $\xi$ ) [6]. This one is defined thanks to the shift factor ( $\Phi$ ), which is the ratio of the actual viscosity ( $\eta$ ) and the viscosity ( $\eta_{ref}$ ) at the reference temperature ( $T_{ref}$ ):

$$d\xi = \Phi(T)dt \text{ and } \Phi(T) = \frac{\eta(T)}{\eta_{\text{ref}}}. \quad (3)$$

The temperature dependence of the viscosity is assumed to follow a Vogel-Fulcher-Tamman law [7] (eq. (7)).

**Structural relaxation.** The structural relaxation is a direct consequence of the thermodynamical definition of glass: the structural state of glass depends on the cooling rate during thermal tempering. This phenomenon is taken into account thanks to the concept of fictive temperature ( $T_f$ ), which represents the temperature of the liquid which is in the same structural state as the considered glass at the temperature ( $T$ ) [8]. By analogy with the viscous relaxation, a response function  $M_v(\xi)$  is defined and expanded into Prony's series [4]. This function allows the definition of the variation of fictive temperature with time:

$$T_f(t) = T(t) - \int_0^t M_v[\xi(t) - \xi(t')] \frac{dT(t')}{dt'} dt' \quad (4)$$

$$M_v(\xi) = \sum_{i=1}^n w_{si} \exp\left(-\frac{\xi}{\tau_{si}}\right). \quad (5)$$

All the temperature dependant parameters are function of the fictive temperature. The thermal expansion is:

$$\varepsilon_{\text{th}} = \beta_g(T(t) - T_f(t)) + \beta_l(T_f(t) - T_0). \quad (6)$$

**Thermomechanical properties of sodalime glass.** All the parameters of the presented model were identified by Saint-Gobain Recherche, they are given in [2] and in the following equations and tables (2 and 3).

Young's modulus E (GPa)	Poisson ratio $\nu$	$K_e / K_g$	$\beta_g$	$\beta_l$
$-4.916 \cdot 10^6 T + 7.1 \cdot 10^{10}$ if $T < 824.4$ K $-3.61 \cdot 10^7 T + 9.67 \cdot 10^{10}$ if $T > 824.4$ K	0.22	0.3	$9 \cdot 10^{-6} \text{ } ^\circ\text{K}^{-1}$	$32 \cdot 10^{-6} \text{ } ^\circ\text{K}^{-1}$

**Table 2.** Thermomechanical properties of glass

i	1	2	3	4	5	6
$w_{li}$	0.0427	0.0596	0.0877	0.2554	0.2901	0.2498
$\tau_{li}$ (s)	19	291.9	1843	11800	49490	171700

**Table 3.** Viscous and structural relaxations - weights and relaxation times ( $T_{\text{ref}} = 776.51$  K)

$$\log(\eta) = -2.74 + \frac{4520}{(T - 525)} \text{ (Pa.s)}. \quad (7)$$

$$w_{2i} = w_{si} = w_{li}; \tau_{2i} = 6 \tau_{li}; \tau_{si} = 9 \tau_{li}. \quad (8)$$

### Identification of heat transfer phenomena during tempering

In the tempering of glass, and rather in the generation of residual stresses, temperature plays a crucial role. Heat exchanges are made by conduction, thermal radiation and convection. The conductive flux ( $\Phi_c$ ) follows the Fourier law:

$$\Phi_c = -\lambda(T) \text{ grad } T. \quad (9)$$

The thermal properties vary with temperature. The temperature dependencies were identified by Saint-Gobain Recherche, they are given in Table 4 and [2].

The cooling by air casts is modelled by a forced convection. Far away from edges, the forced convection is characterised by a heat transfer coefficient and by the air temperature. For the modelling of the tempering of holed plates, several coefficients are defined (in the hole, on the straight edges...). In addition, because of the high temperature at the beginning of the tempering process, the modelling of the thermal radiation is necessary.

Thermal conductivity $\lambda$ (W / m.K, T in K)	Specific heat of liquid glass $C_{p,l}$ (J / kg.K, T in K)	Specific heat of glass $C_{p,g}$ (J / kg.K, T in K)
$0.975 + 8.58 \cdot 10^{-4}(T-273)$	$1433 + 6.5 \cdot 10^{-3} T$	$893 + 0.4 T - 1.8 \cdot 10^{-7} / T^2$

**Table 4.** Thermal conductivity and specific heat of glass

**Thermal radiation modelling.** Radiation is a complex phenomenon in glass which is a semi-transparent medium since infrared waves are not stopped by the first molecular layers they meet, as opposite to the other opaque materials of civil engineering: steel, concrete, timber... [9].

The radiation modelling for the infinite plate is done as follows. The radiative flux is split into two fluxes which emanate from surfaces on one hand, and from the volume on the other hand. Thus, surface and volume emissivities of glass plates are defined in the following way:

- the surface emissivity ( $\varepsilon_{\text{surf}}$ ) is defined for the spectral field where glass is opaque, the radiative transfers take place only on the surface;
- the volume emissivity ( $\varepsilon_{\text{vol}}$ ) is defined for the spectral field where glass is semi-transparent, the radiative transfers occur in all the volume of glass.

It is assumed that radiative transfers take place in a uniform way in all the volume. The surface flux is given by:

$$\Phi_s = 2 \sigma [\varepsilon_{\text{surf}}(T_s)T_s^4 - \varepsilon_{\text{surf}}(T_{\text{ext}})T_{\text{ext}}^4]. \quad (10)$$

Where  $T_s$  is the surface temperature,  $T_{\text{ext}}$  the environment temperature, and  $\sigma$  the Stefan-Boltzmann coefficient. The factor 2 represents the heat exchanges of the two faces of the plate. The volume flux is given by:

$$\Phi_v = 2\sigma [\varepsilon_{\text{vol}}(e, T_v)T_v^4 - \varepsilon_{\text{vol}}(e, T_{\text{ext}})T_{\text{ext}}^4]. \quad (11)$$

Where  $T_v$  is the mean temperature in the thickness ( $e$ ) of the glass plate. The factor 2 is due to the heat exchanges with the two semi-spaces above and under the plate. It is then assumed that each point of the volume only exchanges radiative energy with outside, and not with the neighbouring points within the volume. The surface and volume emissivities were numerically identified from experimental results, they must be considered as apparent emissivities of flat glass [10]. The numerical results for the two emissivities are put into polynomial forms which are easy to handle with the FE code Abaqus. On each Gauss point ( $i$ ), the emitted radiative flux (respectively

absorbed) is calculated by multiplying the volume emissivity by  $(\sigma T_i^4)$  (respectively  $\sigma T_{ext}^4$ ) divided by the thickness of the glass plate. On the surface, the flux corresponding to the opaque spectral field, which results from a similar calculation with the surface emissivity, is added.

**Questions.** The two main assumptions are now discussed for the 19 mm thick glass plates: the uniform radiative exchanges in the volume and the 1D expressions of emissivities. The insight penetration of a radiation doesn't pass from zero to all the volume. In fact, the reduction of the radiation intensity (I) follows an exponential law:

$$I = I_0 \cdot \exp(-K_\lambda x_2). \quad (12)$$

Where  $K_\lambda$  is the absorption factor and  $x_2$  is the thickness coordinate.

Assuming uniform radiative exchanges in the volume is correct for thin glass plates, is it still valid for thick plates ?

The emissivities are determined for infinite plates. In the vicinity of edges and holes, their expressions are theoretically not the same (the problem to solve is 3D). Is it possible to use 1D expressions of emissivities, kept constant in the vicinity of edges and holes ?

**Validation of the modelling.** These two assumptions were checked thanks to experimental results. 250x250x19 mm<sup>3</sup> glass plates, perforated or not, were heated to temperatures where the thermal radiation is very present. Then, they were cooled by natural convection in order to give the importance to the radiation compared to the convection.

During the cooling, the plate were observed with an Infra-Red camera. A 5 $\mu$ m filter was used in order to record the radiation emitted by the surface only because glass can be considered as opaque for this wavelength. This information allowed the determination of the surface temperature.

Residual stresses depend on the history, during the cooling, of the difference between the surface and the volume temperatures within the plate. They are measured by photo-elastic methods: the surface residual stresses are obtained with the Epibiascope which sends a ray of light in a parallel direction to the surface and which uses the "mirage" effect on the tin side [11]. With conventional photo-elastic analysis (transmitted light), it is possible to obtain the membrane stress ( $\Sigma$ ) defined as:

$$\Sigma = \frac{1}{e} \int_{-e/2}^{e/2} (\sigma_{33}(x_2) - \sigma_{11}(x_2)) dx_2. \quad (13)$$

Where  $x_2$  is the thickness coordinate. This one can be neglected everywhere in the plate except near the edge and the hole, where the normal stress is equal to zero.

The numerical simulation of the natural convection tests, taking into account the IR radiation, allows to find the temperature on different points of the plate (far away and in the area of edges and holes). The comparisons between experimental and numerical predictions of surface temperatures was excellent (not shown). The good agreement, shown in Table 5, between the experimental and predicted values of residual stresses validates the calculation of temperatures on every point within the plate. The results obtained far away the edges and the hole assure that the radiative transfers can be considered as uniform in all the volume, whereas the results near the edges and in the vicinity of hole validate the 1D expressions of the emissivities in these 3D area.

	Experimental (MPa)	Calculated (MPa)
Inner surface stress far from the hole and the edge	-67.4	-69.4
Membrane stress close to the edge	-94.4	-91.8
Surface stress close to the hole	-73.2	-74.4

**Table 5.** Comparisons between experimental and calculated residual stresses in different locations of the plate

**Identification of forced convection coefficients.** The convection coefficients in the different area of perforated plates are identified using a hollow aluminium model representative of the external surface of a  $400 \times 400 \times 19$  mm<sup>3</sup> holed glass plate. Fig. 3 and 4 show this model. Each aluminium element (on the edge, on the plate surface, different faces of the hole) is isolated from the others thanks to PTFE washers. All of them are instrumented with thermocouples distributed everywhere on the perforated plate.



**Fig. 3.** The holed model b2



**Fig. 4.** Zoom on the constituents of the chamfered hole

The model is then submitted to real conditions of tempering but is heated to a temperature such as the radiation is negligible. The temperature is recorded thanks to the thermocouples during the cooling process.

Neglecting the conduction term in the heat equation (the aluminium conductivity is very high, so the temperature gradient through the thickness is low), the temperature is given by [12]:

$$d\rho c_p \frac{dT}{dt} = h(T_{\text{air}} - T). \quad (14)$$

Where  $d$  is the thickness of the plate,  $\rho c_p$  the thermal capacity,  $h$  the convection coefficient and  $T_{\text{air}}$  the air temperature. Assuming that  $h$  et  $c_p$  are constant, the previous equation gives the time dependence of temperature:

$$T = (T_0 - T_{\text{air}}) \exp\left(-\frac{ht}{d\rho c_p}\right) + T_{\text{air}}. \quad (15)$$

Where  $T_0$  is the initial temperature. The actual forced convection coefficients on different locations where the temperature is recorded is then given by:

$$h = -\frac{1}{t} d\rho c_p \ln\left(\frac{T - T_{\text{air}}}{T_0 - T_{\text{air}}}\right). \quad (16)$$

All the identified coefficients are given in Table 6.

Plate faces (W/m <sup>2</sup> K)		Chamfered zones (W/m <sup>2</sup> K)			Cylindrical zones (W/m <sup>2</sup> K)		Edges (W/m <sup>2</sup> K)
Far away from the hole	Close to the hole	b1	b2	c1	a1	a2	
77	72	74	78	75	58	61	62

**Table 6.** The different values of the identified forced convection coefficients

### Calculation of residual stresses

**Validation.** All the heat transfers are now identified. The accurate prediction of the residual stresses due to the tempering of thick perforated glass plates is then possible.

The two emissivities model is used to account the thermal radiation. The convection coefficients are those identified with the previous experiments. The initial temperature is given by the manufacturer (630°C). The air temperature was measured during the previous experiments (20°C). The finite element modelling of the thermal process is assumed to be axisymmetric since the thermocouples reveal the cooling symmetries between all the points of the hollow model.

50 tempered perforated glass plates were analysed. Their residual stresses were determined in order to check the FE simulation. The comparisons are made on two different points:

- the surface stresses far away from the hole and the edge; they were obtained thanks to the photo-elastic measurements with an Epibiascope,
- the membrane stresses in the vicinity of the hole and the edge were measured with the transmitted light (the hole is full of a liquid of same refraction index as glass).

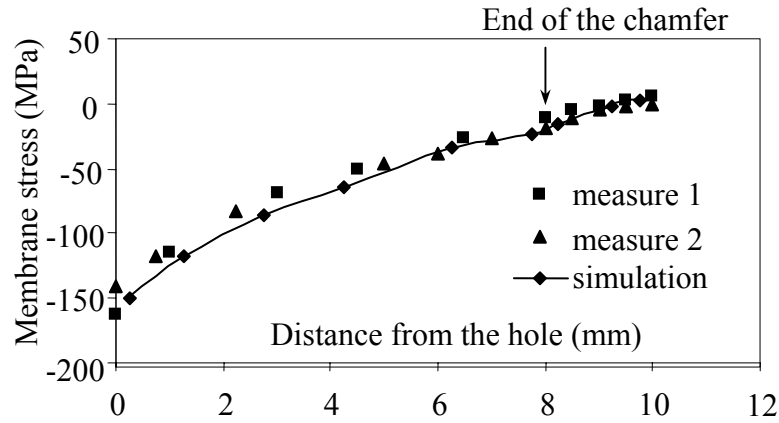
An estimation of these stresses lower than 10 percent, with a maximum of 10 MPa is then obtained.

Table 7 and Fig. 5, 6 show the good agreement between calculated and measured stresses on the samples. It concludes the validation of the thermal tempering modelling.

This simulation can now be used in order to identify the hole geometry which obtains the best reinforcement after tempering.

Measured with the Epibiascope	Simulation
-147 MPa	-144 MPa

**Table 7.** Comparisons between predicted and measured surface stresses



**Fig. 5.** Comparisons between predicted and measured membrane stresses in the vicinity of the hole (for a hole with a large chamfer)

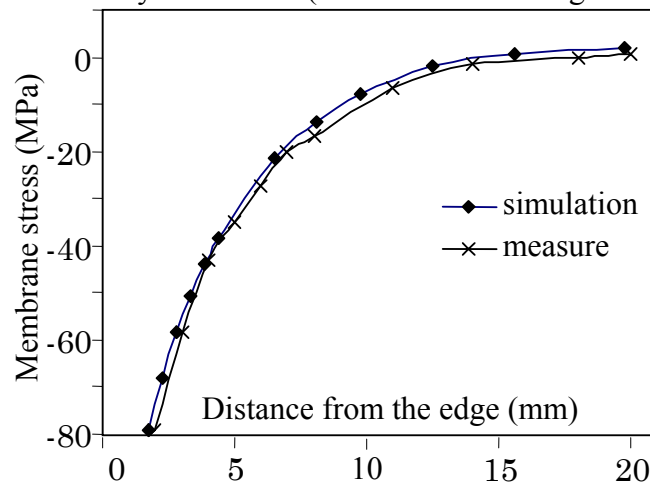


**Fig. 6.** Comparisons between predicted and measured membrane stresses close to the straight edge (the measures started from the chamfer)

**Application of the simulation.** The considered criteria for the analysis of the reinforcement are:

- the surface tangential stresses in the hole,
- the membrane stresses in the vicinity of the hole,
- the neutral line: beyond this line, a zone of integrated tension occurs, that may weaken the hole,
- the compression thickness in the vicinity of the hole.

All the comparisons for the five different hole geometries of this study are grouped together in Fig. 7, 8 and in Table 8. These results allow to conclude that the best reinforcement is obtained for the two holes with large chamfers. The tempering process is the most effective for these kinds of geometry.

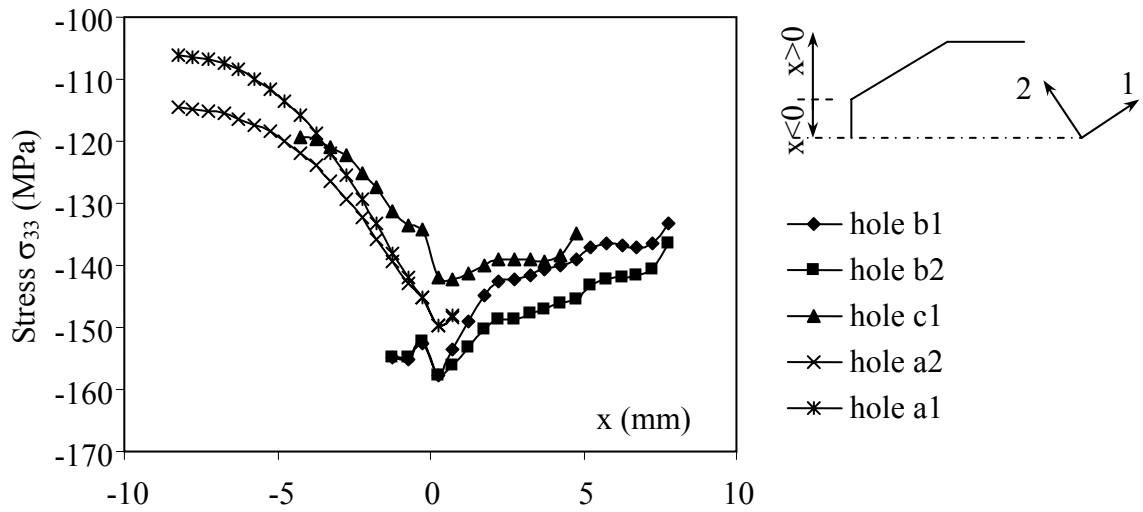


**Fig. 7.** Predicted surface stress  $\sigma_{33}$  for each kind of hole geometry

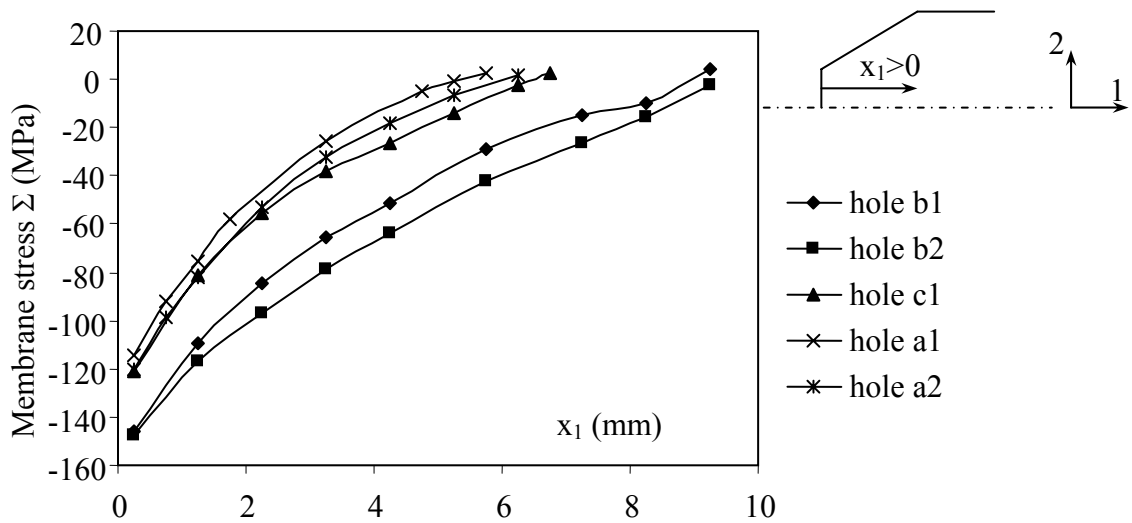


**Fig. 8.** Predicted membrane stress  $\Sigma = \frac{1}{e} \int_{-e/2}^{e/2} (\sigma_{33}(x_2) - \sigma_{11}(x_2)) dx_2$  for each kind of geometry

Type	Surface stress $\sigma_{33}$ (MPa)			Membrane stress (for $x_1=0$ ) (MPa)	Neutral line position (mm)	Compression thickness (mm)
	Min.	Average	Max.			
a1	-106.1	-123	-149.8	-119.6	5.38	3.00
a2	-114.6	-127.7	-149.7	-125.1	6.08	3.35
b1	-133.1	-143.8	-157.6	-155.2	8.94	3.70
b2	-136.6	-147.9	-157.7	-155.6	9.49	4.00
c1	-119.2	-133.1	-142.4	-131.4	6.50	3.64

**Table 8.** Summary table of the predicted results

### Conclusion

The determination of the load-bearing capacity of joints in tempered glass structures passes first by the finite element computation of residual stresses near holes. In this analysis, the heat transfers occurring during tempering play a crucial role, in particularly thermal radiation and forced convection. The thermal radiation is taken into account with the two emissivities method. The

pertinence of this modelling for structural glass is experimentally proved. The actual forced convection coefficients are identified thanks to a hollow aluminium model submitted to real conditions of tempering. These coefficients are different far away and in the vicinity of edges and hole. The identification of these heat exchanges, with the use of the Narayanaswamy's mechanical behaviour model, allows us to conclude that the tempering process is the most effective for holes with large chamfers.

## References

- [1] O.S. Narayanaswamy, R. Gardon: J. Am. Ceramic Society Vol. 52-10 (1969), p. 554-558.
- [2] H. Carré, L. Daudeville: ASCE J. of Eng. Mech. Vol. 125-8 (1999), p. 914-921.
- [3] W. Laufs, G. Sedlacek: Glass Science and Technology Vol. 72-1 (1999), p. 1-14.
- [4] O.S. Narayanaswamy: J. Am. Ceramic Society Vol. 54-10 (1971), p. 491-498.
- [5] R. Gy, L. Duffrene and M. Labrot: J. Non-Cryst. Solids Vol. 175 (1994), p. 103-117.
- [6] F. Schwarzl, A.J. Staverman: J. Applied Physics Vol. 23-8 (1952), p. 838-843.
- [7] L. Duffrene: Ph.D. Thesis (Ecole Nationale Supérieure des Mines de Paris, France 1994).
- [8] A.Q. Tool: J. Am. Ceramic Society Vol. 29-9 (1946), p. 240-253.
- [9] D. Banner: Ph.D. Thesis (Ecole Centrale de Paris, France 1990).
- [10] D. Banner, S. Klarsfeld: *Influence of composition upon the apparent conductivity and emissivity of glass as a function of thickness and temperature* (Thermal conductivity 21, edited by Cremers and Fine, Plenum Press, New York USA 1990).
- [11] H. Aben, C. Guillemet: *Photoelasticity of Glass* (Springer-Verlag, Berlin Germany 1993).
- [12] J.P. Holman: *Heat Transfer* (McGraw-Hill 7<sup>th</sup> ed., USA 1992).